



## Design and Simulation of an Ion Sensitive Field Effect Transistor (ISFET) Readout Circuit, with Low Thermal Sensitivity

---

Abdelkhalak Harrak and Salah Eddine Naimi

EasyChair preprints are intended for rapid dissemination of research results and are integrated with the rest of EasyChair.

January 28, 2020

# Design and Simulation of an Ion Sensitive Field Effect Transistor (ISFET) Readout Circuit, with Low Thermal Sensitivity

Abdelkhalak HARRAK<sup>1\*</sup> and Salah Eddine NAIMI<sup>1</sup>

<sup>1</sup>SDMN Team, ERSETI Laboratory, ENSA, Mohammed First University. BP 669, Oujda  
60000, Morocco

{a.harrak, s.naimi}@ump.ac.ma

**Abstract** Ion Sensitive Field Effect Transistor (ISFET) is one of the biological and/or chemical sensors compatible with the CMOS technology. The sensitivity of the ISFET is measured connecting the device to a readout circuit that provides an output voltage related to the threshold voltage shift according to the ion concentration. However, the influence of the temperature on the whole system (Electrolyte-ISFET-Readout circuit) is critical for proper processing. The proposed readout circuit tends to minimize the thermal sensitivity of the sensor circuit. The simulation was done using the AMI 1 $\mu$ m CMOS process provided by MOSIS, while the Verilog-A was used to model a pH-ISFET behavior. Simulation results with 3V supply voltage and a temperature range from 20°C to 80°C, shows a pH sensitivity of 40 mV/pH with thermal sensitivity less than 0.0005517pH/°C. The coefficient of determination  $R^2$  is around 0.999984 at  $T = 20^\circ\text{C}$  and quantify the strength of the linear relationship.

**Keywords:** pH-ISFET, Readout-Circuit, Temperature Sensitivity.

## 1 Introduction

The ISFET (Ion-Sensitive Field Effect Transistor) sensor was invented by Bergveld in the early 1970s [1]. Since its first apparition, its structures knew many developments and ameliorations in several domains, such as chemical ones which are becoming more popular for measuring ionic concentrations of electrolyte solutions [2, 3]. Showing remarkable capability for biochemical analysis, the ISFET may be used to identify glucose, proteins and hormones [4]. It has attracted a considerable attention in most research, its integration with CMOS technology makes it very cheap. His capacity to operate under low voltage with low power consumption allows him to meet the demand for low-voltage and low-power systems. Recently, it has been confirmed that the pH-ISFET sensor can be fabricated using a series of industrial CMOS technologies [4,5]. Despite the advantages of the ISFET sensor, it requires more investigation to decrease the temperature sensitivity, the body effect concerns and the device mismatch, due to the process variation, which are the major problems for precision circuit design. Most recent researches in the field have made to develop temperature compensation techniques in order to achieve more stable ISFETs sensors [6,7]. Complex architecture circuits have shown the best results. Develop a simple analog circuit that can support all the constraints mentioned previously is a challenge [8]. In this paper, we propose a relatively simple analog readout circuit associated with a CMOS compatible pH-ISFET structure. To feed the proposed readout circuit, we have chosen a modified Widlar current source that shows good stability and low-

temperature sensitivity than an ordinary current source. The readout circuit is simulated to verify the temperature dependency advantages.

## 2 The pH-ISFET structure

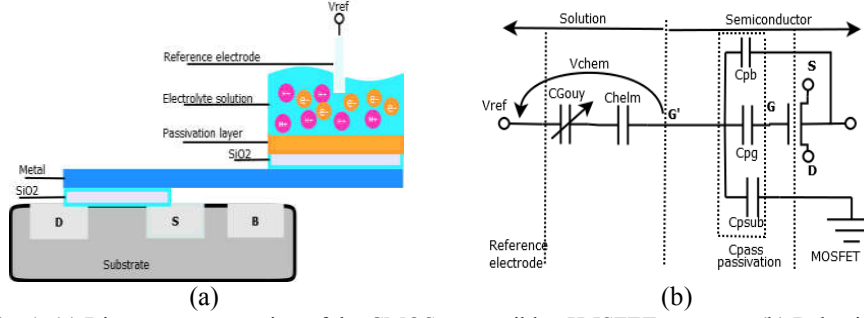


**Fig. 1.** (a) Diagram cross-section of the CMOS compatible pH-ISFET structure, (b) Behavioral macro model of the structure in (a)

The schematic illustration exposed by Fig. 1a, shows the structure of the CMOS compatible, ion sensitive field effect structure (ISFET). It is the same as the MOSFET structure, except that the gate insulation is exposed to the fluid. The metal gate is thus replaced by a reference electrode (typically Ag/AgCl) emerged in an electrolyte and the gate dielectric replaced by a sensitive membrane such as silicon nitride. The typical structure, shown in Fig. 1a constrained to make the passivation gate far to the gate of the MOSFET, by connecting them with a metal, to avoid the influence of the trapped charge between the passivation layer source and passivation layer-drain. As it can be seen, the integration with semiconductor technologies allows building different sensors such as pH-ISFETs, BioFETs and REFETs, by a simple change in the sensitive membrane. The macro-model of the presented structure is shown in Fig. 1b. The well-known site binding theory combined to the Gouy-Chapman-Stern double-layer model and the standard model of the MOSFET transistor (BSIM3v3) contribute developing a robust behavioral model of the ISFET. The threshold voltage of the ISFET is the sum of the threshold voltage of the MOSFET and some potential ( $V_{chem}$ ) across the electrolyte.

$$V_{TH}(ISFET) = V_{TH}(MOSFET) + V_{chem} \quad (1)$$

As provided in [4], the  $V_{chem}$  voltage expression, which depends on the pH of the electrolyte, is shown in (2).

$$V_{chem} = E_{ref} - \psi_0 + \chi_{sol} - \frac{\phi_m}{q} \quad (2)$$

Where  $E_{ref}$ ,  $\psi_0$ ,  $\phi_m$ ,  $\chi_{sol}$  and  $q$  are respectively, the relative potential of the reference electrode, the potential drop in the electrolyte at the insulator-electrolyte interface, the electron work function at the gate metal, the electrolyte-insulator surface dipole potential with a typical value of 50mV and the electron charge. In Eq. (2),  $\psi_0$  is

the only parameter responsible for the ISFET pH sensitivity, as explained by the site binding theory. The expression of the surface potential from (2) is as follow:

$$\psi_0 = \frac{q}{C_{eq}} \left[ N_{sil} \left( \frac{\exp\left(\frac{-2\psi_0}{U_T}\right) - \exp(\log(K_a \times K_b) + 4.6pH)}{\exp\left(\frac{-2\psi_0}{U_T}\right) + \exp(\log(K_a) + 2.3pH) \exp\left(\frac{-\psi_0}{U_T}\right) + \exp(\log(K_a \times K_b) + 4.6pH)} \right) + qN_{nit} \left( \frac{\exp\left(\frac{-\psi_0}{U_T}\right)}{\exp\left(\frac{-\psi_0}{U_T}\right) + \frac{K_n}{K_a} \exp(\log(K_a) + 2.3pH)} \right) \right] \quad (3)$$

With

$$C_{eq} = C_{gouy} C_{Helm} / (C_{gouy} + C_{Helm}) \quad (4)$$

The surface potential of the sensitive membrane (in case of  $Si_3N_4$ ), is modeled using a double sites theory. In equation 3,  $N_{sil}$  is the density of silanol sites,  $N_{nit}$  the density of amine sites.  $U_T$  the thermal voltage,  $k_a$ - $k_b$  and  $k_n$  are the dissociation constants of the chemical reactions at the insulator interface. The capacitances,  $C_{gouy}$  and  $C_{helm}$  are related to the Gouy-Chapman-Stern double-layer model. The expression of the potential surface considers the second order phenomena to allow a realistic behavior of the sensors with the temperature. The model have been implemented in Verilog-A. The passivation capacitances,  $C_{pg}$ ,  $C_{psub}$  and  $C_{pb}$ , are the gate passivation, substrate passivation and bulk passivation capacitances, respectively, they are associated to the two dielectrics  $Si_3N_4$  and  $SiO_2$ , these capacitances could be calculated by the following equation:

$$C_{pass} = (w * l)_{chem} \epsilon_0 \frac{\epsilon_{Si_3N_4} \epsilon_{SiO_2}}{\epsilon_{Si_3N_4} \cdot t_{SiO_2} + \epsilon_{SiO_2} \cdot t_{Si_3N_4}} \quad (5)$$

The term  $(w * l)_{chem}$  in (5) is a geometric parameter that depends on the layout of the floating gate.  $\epsilon_0$ ,  $\epsilon_{Si_3N_4}$  and  $\epsilon_{SiO_2}$  are the permittivity of a free space, silicon nitride and silicon dioxide, respectively.  $t_{Si_3N_4}$  and  $t_{SiO_2}$  are the thickness of the silicon nitride and the silicon oxide, respectively. The passivation characteristics are considered as big problem in ISFETs sensors, we distinguish two main axes of this problem. First, the trapped introduced charge in the passivation layer [4, 9, 10], will creates a threshold voltage offset that will influence in the readout circuit and that is due to the fabrication methods after membrane sensible deposition (a silicon nitride in our ISFET). Due to passivation dielectric, which creates depletion charge next to the drain and source, this later comes back to the passivation layer deposition in the gate of the MOSFET. To resolve depletion charge and as shown in Fig. 1a, we have pushed the passivation layer by a metal beside the gate of the MOSFET, without contact with the latest. The trapped charge can be removed by the UV radiation as mentioned in [4]. The effective weak inversion slop factor  $n$  of the MOSFET part of the ISFET is directly influenced by all these capacitances. The slop factor  $n$  is given by the formula below [4].

$$n = 1 + \frac{C_d}{C_{ox} // C_{pass} // C_{gouy} // C_{helm}} \quad (6)$$

Where  $C_d$ ,  $C_{ox}$  are respectively, the depletion and the oxide capacitances.

### 3 The readout circuit of the ISFET

To improve the output response of the ISFET structure, lot of circuits had been presented in the literature, as mentioned in [11]. The proposed circuit is composed of four stages as shown in Fig. 2, the Caprio's quad which allows extracting the threshold voltage shift of the ISFET, two attenuators and voltage shifter who will adapt the signal to the next stage, a differential amplifier and current sources.

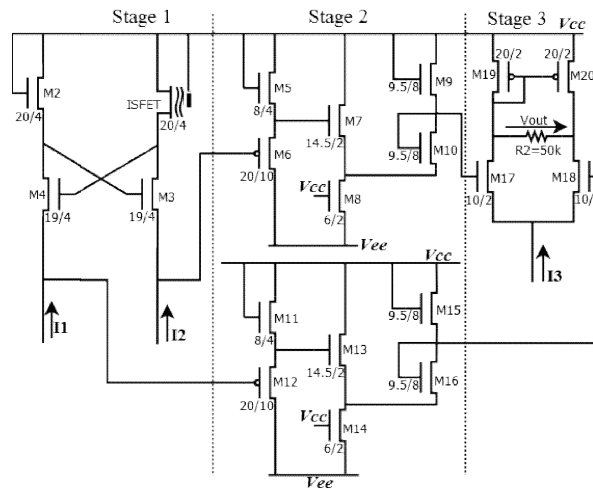


**Fig. 2.** The readout circuit, stage 1: Caprio's quad, stage 2 : attenuators, stage 3 : differential amplifier

The role of each stage in the proposed circuit was explained and developed in [8, 12].

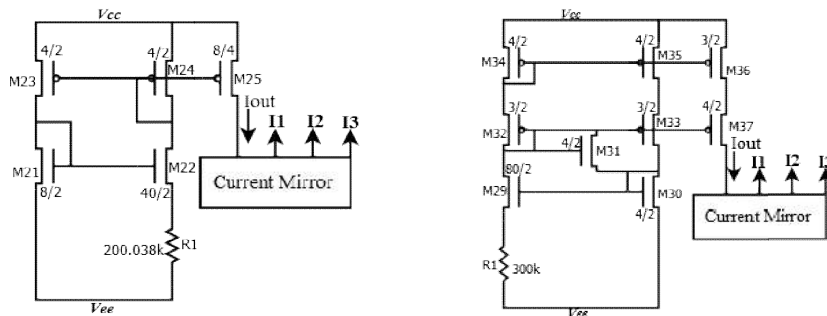


**Fig. 3.** On the left, the standard Wildar current source, on the right, an improved Wildar current source from [13]

The current source is one of the key elements for building a robust analog readout circuit. We took advantage of the wealth of the existing current sources in the literature to make a comparative study of two current sources, as shown in Fig. 3. The out-

put of the current source is connected to a cascode current mirror, which supplies the currents  $I_1$ ,  $I_2$  and  $I_3$  to the readout circuit presented in Fig. 2.

#### 4 Simulation results and discussion

In order to validate the model of the pH-ISFET, and to estimate the effect of the temperature on the output of the sensor, the threshold shift of the pH-ISFET was simulated for a pH of the electrolyte varying from 1 to 12. The results in Fig. 4, shows that unfortunately, the output of the pH-ISFET gives a very large variation with the temperature around  $0.097 \text{ pH}/^\circ\text{C}$ . The characteristics still show a high linearity response.

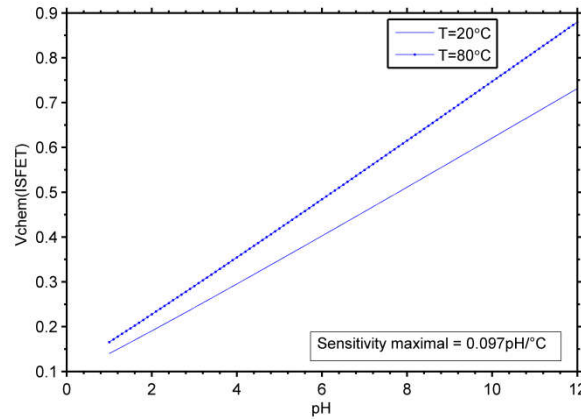
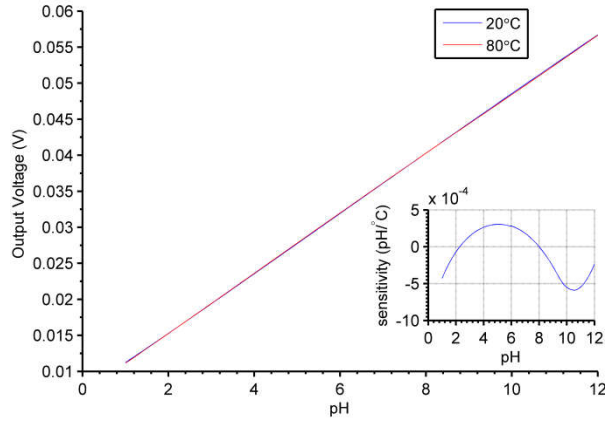


Fig. 4. ISFET macro model output response

The simulation results of the temperature sensitivity of current sources, as well as the output response of the readout circuit, are presented in Fig. 5 and table 1. Both Widlar sources were designed to achieve a required current around  $7.3 \mu\text{A}$ . The transistors sizes ( $W/L$  ( $\mu\text{m}/\mu\text{m}$ )) are shown in the circuits. As can be shown, the modified Widlar source is less sensitive to the variation of the temperature compared to the standard Widlar circuit. The output response of the readout circuit has a very good linearity, confirmed by the values of the coefficient of determination of the regression  $R^2$  ( $R^2=0.999893$  and  $0.999927$  for a temperature  $T=20^\circ\text{C}$  and  $80^\circ\text{C}$  respectively). The maximum temperature sensitivity of the readout circuit output is around  $0.00055 \text{ pH}/^\circ\text{C}$  when a modified Widlar source is used, while it remains about  $0.00076 \text{ pH}/^\circ\text{C}$  for the standard Widlar source.



**Fig. 5.** Final simulation of the readout circuit and the temperature sensitivity

**Table 1.** pH sensing properties and electrical characteristics of the readout circuit for both current sources

	Standard Wildar current source	Modified Wildar current source
Maximum sensitivity of the readout circuit output (pH/°C)	0.00076	0.00055
Current source sensitivity ( $\mu A/^\circ C$ ) for $I_{out}=7.3\mu A$	0.00953	0.00701

## 5 Conclusion

In this work, an analog readout circuit adapted to a CMOS compatible pH-ISFET sensor was proposed. The behavioral model of the pH-ISFET was elaborated using a site binding theory combined with the Gouy-Chapman-Stern double-layer model. The  $Si_3N_4$  material with double sites was considered as a sensitive membrane in the simulation. A behavioral model of the sensor was implemented in Verilog-A. Our main goal has been focused to perform a linear and temperature insensitive readout circuit for the pH-ISFET. Two approaches of the current source needed in our readout circuit were studied. A modified Widlar source was able to improve the temperature sensitivity of the output, we got a simulated shift of about  $0.00055 \text{ pH}/^\circ C$  for pH of 10.6 and only  $0.000006 \text{ pH}/^\circ C$  for pH = 8. In addition, the linearity of the output is very good at a range of temperature from 20 to  $80^\circ C$ , the estimated coefficient of determination of the regression  $R^2$  was about 0.9999.

## References

1. Bergveld, P.: Short Communications: Development of an Ion-Sensitive Solid-State Device for Neurophysiological Measurements. IEEE Trans. Biomed. Eng. BME-17, 70–71 (1970).

doi:10.1109/TBME.1970.4502688

2. Bergveld, P.: Thirty years of ISFETOLOGY. *Sensors Actuators B Chem.* 88, 1–20 (2003). doi:10.1016/S0925-4005(02)00301-5
3. Garner, D.M., Bai, H., Georgiou, P., Constandinou, T.G., Reed, S., Shepherd, L.M., Wong, W., Lim, K.T., Toumazou, C.: A multichannel DNA SoC for rapid point-of-care gene detection. *Dig. Tech. Pap. - IEEE Int. Solid-State Circuits Conf.* 53, 492–493 (2010). doi:10.1109/ISSCC.2010.5433834
4. Georgiou, P., Toumazou, C.: ISFET characteristics in CMOS and their application to weak inversion operation. *Sensors Actuators, B Chem.* 143, 211–217 (2009). doi:10.1016/j.snb.2009.09.018
5. Hammond, P.A., Ali, D., Cumming, D.R.S.: Design of a Single-Chip pH Sensor Using a Conventional 0.6- $\mu$ m CMOS Process. *IEEE Sens. J.* 4, (2004). doi:10.1109/JSEN.2004.836849
6. Chin, Y.-L., Chou, J.-C., Sun, T.-P., Chung, W.-Y., Hsiung, S.-K.: A novel pH sensitive ISFET with on chip temperature sensing using CMOS standard process. *Sensors and Actuators B.* 76, 582–593, (2001). doi:10.1016/S0925-4005(01)00639-6
7. Chung, W.-Y., Lin, Y.-T., Pijanowska, D.G., Yang, C.-H., Wang, M.-C., Krzyskow, A., Torbicz, W.: New ISFET interface circuit design with temperature compensation. *Microelectronics J.* 37, 1105–1114 (2006). doi:10.1016/j.mejo.2006.05.001
8. Harrak, A., Naimi, S.E.: Design and simulation of low power CMOS compatible pH-ISFET readout circuit, with low thermal sensitivity. *IEEE Xplore.* 1, 1–6 (2017). doi:10.1109/EITech.2017.8255263
9. Cané, C., Götz, A., Merlos, A., Gràcia, I., Errachid, A., Losantos, P., Lora-Tamayo, E.: Multilayer ISFET membranes for microsystems applications. *Sensors Actuators B Chem.* 35, 136–140 (1996). doi:10.1016/S0925-4005(97)80043-3
10. Bausells, J., Carrabina, J., Errachid, a, Merlos, a: Ion-sensitive eld-effect transistors fabricated in a commercial CMOS technology. *Sens. Actuators B Chem.* vol, 57no1-3pp56-62 (1999). doi:10.1016/S0925-4005(99)00135-5
11. Moser, N., Lande, T.S., Toumazou, C., Georgiou, P.: ISFETs in CMOS and Emergent Trends in Instrumentation: A Review. *IEEE Sensors Journal.* 6496 -6514 (2016). doi: 10.1109/JSEN.2016.2585920
12. Naimi, S.E., Hajji, B., Humenyuk, I., Launay, J., Temple-Boyer, P.: Temperature influence on pH-ISFET sensor operating in weak and moderate inversion regime: Model and circuitry. *Sensors Actuators, B Chem.* 202, 1019–1027 (2014). doi:10.1016/j.snb.2014.06.008
13. Wang, Y.T., Chen, D., Geiger, R.L.: A CMOS supply-insensitive with 13ppm/°C temperature coefficient current reference. *Midwest Symp. Circuits Syst.* 475–478 (2014). doi:10.1109/MWSCAS.2014.6908455